Inorganic Chemistry
Article

Inorg. Chem. **2010**, *49*, 1679–1686 **1679**
DOI: 10.1021/ic902092e

Facile Fabrication of Hierarchical SnO_2 Microspheres Film on Transparent FTO Glass

Yu-Fen Wang,[†] Bing-Xin Lei,[†] Yuan-Fang Hou,[†] Wen-Xia Zhao,[‡] Chao-Lun Liang,[‡] Cheng-Yong Su,[†] and Dai-Bin Kuang*,[†]

[†]*MOE Key Laboratory of Bioinorganic and Synthetic Chemistry, State Key Laboratory of Optoelectronic Materials and Technologies, School of Chemistry and Chemical Engineering, and* [‡]*Instrumental Analysis and Research Center, Sun Yat-Sen University, Guangzhou 510275, P.R. China*

Received October 22, 2009

Hierarchical SnO_2 microspheres consisting of nanosheets on the fluorine-doped tin oxide (FTO) glass substrates are successfully prepared via a facile hydrothermal synthesis process. The as-prepared novel microsphere films were characterized in detail by X-ray diffraction (XRD), field emission scanning electron microscopy (FE-SEM), transmission electron microscopy (TEM), UV−vis diffuse reflectance spectroscopy. Moreover, SnO_2 nanoparticles with 30−80 nm in size covered on the surface of nanosheets/microspheres were also obtained by optimizing the hydrothermal reaction temperature, time, or volume ratio of acetylacetone/H_2O. The detailed investigations disclose the experimental parameters, such as acetylacetone, NH_4F, and seed layer play important roles in the morphology of hierarchical SnO_2 microspheres on the FTO glass. The formation process of SnO_2 microspheres is also proposed based on the observations of time dependent samples.

Introduction

Nanostructured materials with hierarchical morphology are of particular interest because of their potential applications in nanodevices.[1] Complex three-dimensional (3D) structures or films assembled from well-defined zero-dimensional (0D), one-dimensional (1D), and two-dimensional (2D) structures have received tremendous attention.[2,3] Moreover, a number of functional nano/microdevices based on the assembly of low dimensional nanostructured materials have been variously investigated. Three dimensional microsphere films with hierarchical structures on conductive substrate are desirable for the potential applications in optoelectronics,[4] displays,[5] solar cells,[6] and so forth. However, up to the current date, there are few reports on this issue.

Tin oxide (SnO_2) as an environmentally friendly n-type semiconductor material with a wide direct band gap (E_g = 3.6 eV at 300 K)[7] is a promising multifunctional material with remarkable chemical, electronic, gas-sensing, and optical properties,[8] which has been extensively studied. Recently, SnO_2 has shown great technological applications in gas sensors,[9,10] dye-sensitized solar cells,[11] transistors,[12] electrodes for lithium ion batteries,[13,14] catalyst supports,[15] and supercapacitors.[16] It is well-known that the morphology, size, and structure of a specific material strongly influence the corresponding chemical, physical properties and their practical applications.[7] Considering these extensive applications, a variety of methods have been developed to prepare SnO_2

*To whom correspondence should be addressed. E-mail: kuangdb@mail.sysu.edu.cn.

(1) Tian, N.; Zhou, Z. Y.; Sun, S. G.; Ding, Y.; Wang, Z. L. *Science* **2007**, *316*, 732.
(2) Collins, P. G.; Bradley, K.; Ishigami, M.; Zettl, A. *Science* **2000**, *287*, 1801.
(3) Poncharal, P.; Wang, Z. L.; Ugarte, D.; de Heer, W. A. *Science* **1999**, *283*, 1513.
(4) Shen, G. Z.; Chen, P. C.; Ryu, K. M.; Zhou, C. W. *J. Mater. Chem.* **2009**, *19*, 828.
(5) Morales, A. M.; Lieber, C. M. *Science* **1998**, *279*, 208.
(6) Bergeron, B. V.; Marton, A.; Oskam, G.; Meyer, G. J. *J. Phys. Chem. B* **2005**, *109*, 937.
(7) Caruso, F. *Adv. Mater.* **2001**, *13*, 11.
(8) Peng, X. G.; Manna, L.; Yang, W.; Wickham, J.; Scher, E. *Nature* **2000**, *404*, 59.
(9) Xu, X. X.; Zhuang, J.; Wang, X. *J. Am. Chem. Soc.* **2008**, *130*, 12527.
(10) Epifani, M.; Díaz, R.; Arboil, J.; Comini, E.; Sergent, N.; Pagnier, T.; Siciliano, P.; Faglia, G.; Morante, J. R. *Adv. Funct. Mater.* **2006**, *16*, 1488.
(11) Gubbala, S.; Chakrapani, V.; Kumar, V.; Sunkara, M. K. *Adv. Funct. Mater.* **2008**, *18*, 2411.
(12) Duan, X. F.; Huang, Y.; Cui, Y.; Wang, J. F.; Lieber, C. M. *Nature* **2001**, *409*, 66.
(13) Zhang, W. M.; Hu, J. S.; Guo, Y. G.; Zheng, S. F.; Zhong, L. S.; Song, W. G.; Wan, L. J. *Adv. Mater.* **2008**, *20*, 1160.
(14) Wang, Y.; Wu, M. H.; Jiao, Z.; Lee, Y. J. *Nanotechnology* **2009**, *20*, 345704.
(15) Jiang, L. H.; Sun, G. Q.; Zhou, Z. H.; Sun, S. G.; Wang, Q.; Yan, S. Y.; Li, H. Q.; Tian, J.; Guo, J. S.; Zhou, B.; Xin, Q. *J. Phys. Chem .B* **2005**, *109*, 8774.
(16) Prasad, K. R.; Miura, N. *Electrochem. Commun.* **2004**, *6*, 849.
(17) Juttukonda, V.; Paddock, R. L.; Raymond, J. E.; Denomme, D.; Richardson, A. E.; Slusher, L. E.; Fahlman, B. D. *J. Am. Chem. Soc.* **2006**, *128*, 420.

© 2010 American Chemical Society
Published on Web 01/11/2010

material with various morphologies such as nanoparticles,[17] nanorods,[18,19] nanowires,[20,21] nanotubes,[22,23] microspheres,[24] hollow microspheres,[25,26] nanobelts,[27] nanoribbons,[28] nanosheets,[29] nanodendrites,[30] nanodisks,[31] flowers.[32] However, the design of nanostructured SnO_2 materials with novel and structurally well-defined morphologies, in particular, highly ordered 3D arrays, has been difficult to achieve and remain crucial challenges. Recently, Li[33] reported the SnO_2 microspheres powder prepared via a chemical vapor deposition (CVD) process which needed high temperature and incurred high energy cost. No research revealing the fabrication of hierarchical microspheres consisting of nanosheets on transparent conductive substrate has been reported up to date.

Recently, we have already demonstrated the preparation of hierarchical β-$Ni(OH)_2$ microspheres powder consisting of nanosheets.[34] Here we further report the fabrication of hierarchical SnO_2 microsphere films composed of nanosheets and nanoparticles on fluorine-doped tin oxide (FTO) glass substrate via a controllable hydrothermal process. The formation of hierarchical SnO_2 microspheres is associated with the self-assembled growth of nanosheets in the present acetylacetone (acac) and H_2O system. The prepared hierarchical SnO_2 microspheres films were characterized in detail by scanning electron microscopy (SEM), transmission electron microscopy (TEM), and UV−vis spectra.

Experimental Section

Materials. The chemicals including tin(IV) chloride pentahydrate ($SnCl_4 \cdot 5H_2O$), ammonium fluoride (NH_4F), acetylacetone (acac), and ethanol, and so forth were A.R. reagents and used as received without further purification. The fluorine-doped tin oxide (FTO) conductive glasses were cleaned ultrasonically with diluted acid, ethanol, acetone, and water for 5 min, respectively, and then dried in air.

Synthesis. SnO_2 precursors were simply prepared by mixing tin tetrachloride (0.01 M) and sodium hydroxide (1.00 M) at 40 °C for 30 min under stirring, which was ripened for 8 h, and the product was collected by centrifuging at 5000 rpm for 5 min.[35]

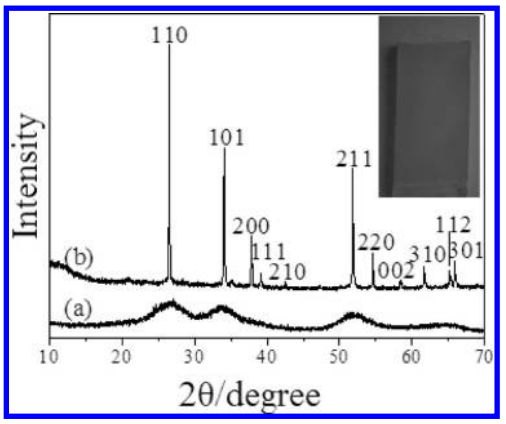

Figure 1. (a) XRD pattern of the SnO_2 seeds, (b) the SnO_2 microspheres synthesized at 180 °C for 24 h with V_{H2O}:V_{acac} = 1:1 (sample **I**, curve b). Inset is the photocopy of sample **I** on FTO glass substrate.

Then, the collected colloids were redispersed into 8 mL of deionized water via ultrasonication for 10 min to obtain a homogeneous suspension. After that, the colloidal precursors were deposited on the FTO substrate via dip-coating as "seed layer". Next, the FTO glass with seed layer was placed into an electronic oven and maintained at 80 °C for 23 h.

In a typical synthesis of hierarchical SnO_2 microspheres, 0.701 g of $SnCl_4 \cdot 5H_2O$ was dissolved in a mixed solvent of 20 mL of deionized water and 20 mL of acac in a 50 mL Teflon-lined stainless steel autoclave. Afterward, 0.444 g of NH_4F was added to this solution under vigorous stirring, continuously stirred for anther 30 min. The FTO glass substrate with "seed layer" was placed at the bottom of the Teflon-lined autoclave. Subsequently, the autoclave was sealed, put into electronic oven, and maintained at 180 °C for 24 h. When the reaction was finished, the autoclave was cooled down to room temperature naturally. The fully covered and homogeneous thin films on FTO glass were thoroughly washed with water and ethanol, and dried at 75 °C for 30 min in air for further characterization. A set of experiments were performed via adjustment of hydrothermal reaction temperature, time, and different ratio of H_2O and acac. Typically, Sample **I**: H_2O/acac = 1:1, 180 °C, 24 h. Sample **II**: H_2O/acac = 1:3, 180 °C, 24 h. Sample **III**: H_2O/acac = 1:1, 200 °C, 24 h. Samples **I**−**III** have the same content of $SnCl_4 \cdot 5H_2O$ (0.701 g) and NH_4F (0.444 g).

Materials Characterization. X-ray Diffraction. The phase purity of the products was characterized by powder X-ray diffraction (XRD) on a Bruker D8 Advance X-ray diffractometer using Cu Kα radiation (λ = 1.5418 Å), with an operating voltage of 40 kV, and a current of 40 mA.

Electron Microscopy. Field emission scanning electron microscopy (FE-SEM, JSM-6330F) were applied to investigate the size and morphology. TEM, high-resolution TEM (HRTEM), and selected area electron diffraction (SAED) patterns were performed on a JEOL-2010 HR transmission electron microscope.

UV. UV−vis diffuse reflectance spectra were measured on a UV−vis−NIR Spectrophotometer (UV, Shimadzu UV-3150).

Results and Discussion

Three dimensional hierarchical SnO_2 microsphere films on FTO glass substrate were obtained via a hydrothermal process. First, the FTO glass dip-coated into a colloid solution containing 0.005 M $SnCl_4 \cdot 5H_2O$ and 0.500 M NaOH to form a SnO_2 seed layer on the surface of FTO glass. Subsequently, hydrothermal synthesis was performed by putting the FTO glass with a seed layer into the Teflon-lined stainless steel autoclave containing $SnCl_4 \cdot 5H_2O$, acac,

(18) Vayssieres, L.; Graetzel, M. *Angew. Chem., Int. Ed.* **2004**, *43*, 3666.
(19) Kuang, Q.; Lao, C. S.; Wang, Z. L.; Xie, Z. X.; Zheng, L. S. *J. Am. Chem. Soc.* **2007**, *129*, 6070.
(20) Wang, Y. L.; Jiang, X. C.; Xia, Y. N. *J. Am. Chem. Soc.* **2003**, *125*, 16176.
(21) Qin, L. P.; Xu, J. Q.; Dong, X. W.; Pan, Q. Y.; Cheng, Z. X.; Xiang, Q.; Li, F. *Nanotechnology* **2008**, *19*, 185705.
(22) Liu, Y.; Liu, M. *Adv. Funct. Mater.* **2005**, *15*, 57.
(23) Lai, M.; Lim, J. H.; Mubeen, S.; Rheem, Y. W.; Mulchandani, A.; Deshusses, M. A.; Myung, N. V. *Nanotechnology* **2009**, *20*, 185602.
(24) Han, S.; Jang, B.; Kim, T.; Oh, S. M.; Hyeon, T. *Adv. Funct. Mater.* **2005**, *15*, 1845.
(25) Yang, H. G.; Zeng, H. C. *Angew. Chem., Int. Ed.* **2004**, *43*, 5930.
(26) Lou, X. W.; Wang, Y.; Yuan, C.; Lee, J. Y.; Archer, L. A. *Adv. Mater.* **2006**, *18*, 2325.
(27) Cheng, B.; Russell, J. M.; Shi, W. S.; Zhang, L.; Samulski, E. T. *J. Am. Chem. Soc.* **2004**, *126*, 5972.
(28) Hu, J. Q.; Bando, Y.; Liu, Q. L.; Golberg, D. *Adv. Funct. Mater.* **2003**, *13*, 493.
(29) Wang, W. W.; Zhu, Y. J.; Yang, L. X. *Adv. Funct. Mater.* **2007**, *17*, 59.
(30) Dai, Z. R.; Pan, Z. W.; Wang, Z. L. *Adv. Funct. Mater.* **2003**, *13*, 9.
(31) Dai, Z. R.; Pan, Z. W.; Wang, Z. L. *J. Am. Chem. Soc.* **2002**, *124*, 8673.
(32) Jiang, L. Y.; Wu, X. L.; Guo, Y. G.; Wan, L. J. *J. Phys. Chem. C* **2009**, *113*, 14213.
(33) Ge, J. P.; Wang, J.; Zhang, H. X.; Wang, X.; Peng, Q.; Li, Y. D. *Sens. Actuators, B* **2006**, *113*, 937.
(34) Kuang, D. B.; Lei, B. X.; Pan, Y. P.; Yu, X. Y.; Su, C. Y. *J. Phys. Chem. C* **2009**, *113*, 5508.
(35) Cao, X. B.; Lan, X. M.; Zhao, C.; Shen, W. J.; Yao, D.; Gao, W. J. *J. Cryst. Growth* **2007**, *306*, 225.

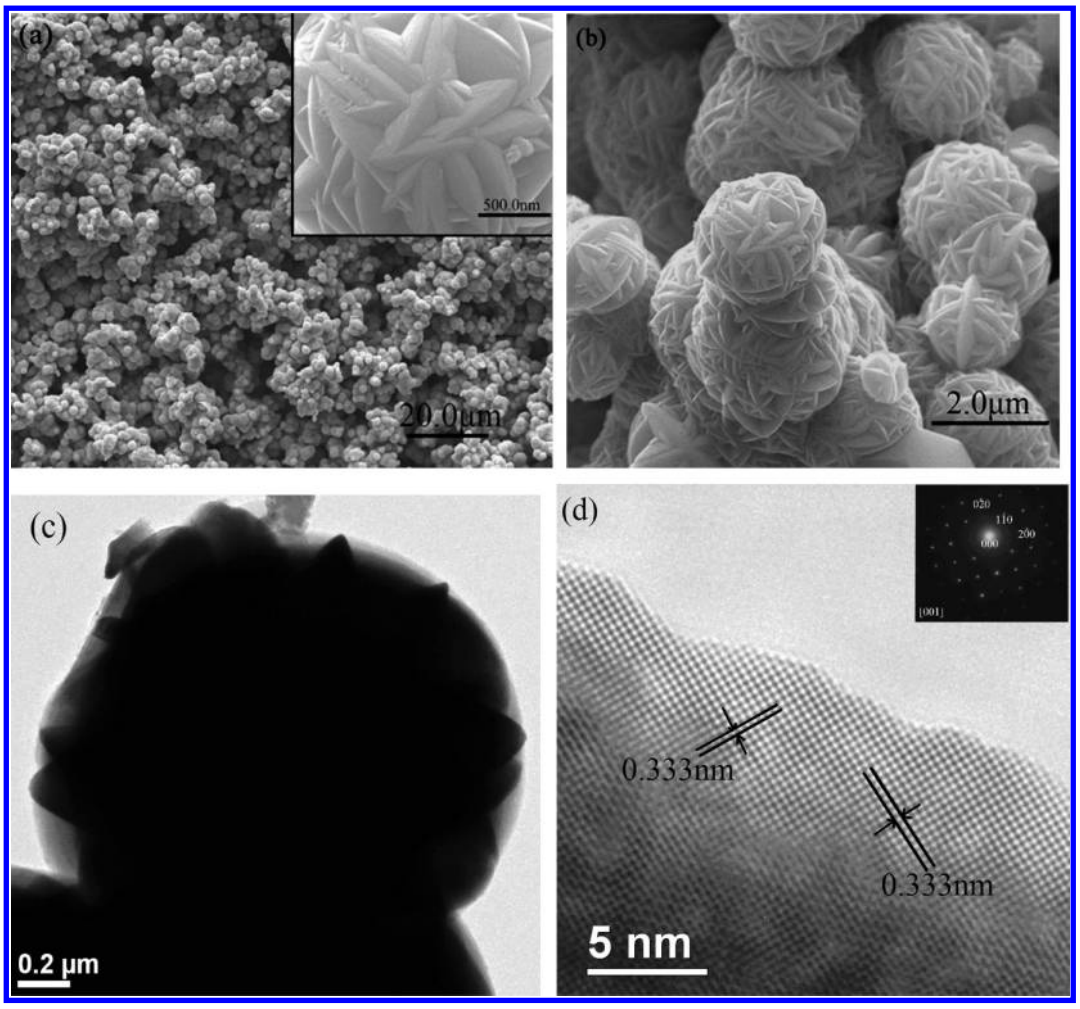

Figure 2. (a, b) FE-SEM images of sample **I** synthesized at 180 °C for 24 h with V_{H2O}:V_{acac} = 1:1. (c, d) TEM and HRTEM images of the typical SnO_2 microsphere and nanosheet (sample **I**), respectively. Inset in Figure 2a is the higher magnification FE-SEM image. Inset in Figure 2d is a typical SAED pattern of an individual nanosheet.

NH_4F, and H_2O, and kept at 160−200 °C for different time (see the experimental details).

The phase composition and structure of the seed layer and the final product after the hydrothermal synthesis were examined by powder XRD. As shown in Figure 1, the seed layer material is of poor crystalline nature which was measured by collection of the seed layer powder (Figure 1a). However, after the hydrothermal reaction, all the reflection peaks of sample **I** (see Experimental Section) can be readily indexed to pure tetragonal phase of SnO_2 (JCPDS Card No. 41-1445) with $a = b = 4.738$ Å and $c = 3.187$ Å, shown in Figure 1b. The stronger peaks of the XRD patterns show that the as-prepared SnO_2 microspheres are highly crystalline. No characteristic peaks from other crystalline impurities were observed, indicating the high purity of the final products. For the seed layer on FTO glass, it is a very thin layer and hard to see clearly by naked eyes. However, after hydrothermal reaction, the photocopy image of sample **I** clearly show that there is a compact material on the FTO glass surface (inset in Figure 1).

The morphology of the synthesized SnO_2 on FTO glass were characterized by field emission SEM (FE-SEM). Figure 2, panels a−b, shows the typical FE-SEM images of sample **I** obtained in mixed solution with V_{H2O}:V_{acac} = 1:1 at 180 °C for 24 h. From the lower magnification FE-SEM image (Figure 2a), it is clearly seen that the surface panoramic morphologies of the products on FTO glass are composed of uniform SnO_2 microspheres. Figure 2b displays these hierarchical SnO_2 microspheres with an average diameter of 2.0−2.5 μm and are composed of numerous nanosheets. The structural details were further shown in the higher magnification FE-SEM image (inset in Figure 2a) and clearly disclosed that the sheets possessed very smooth surfaces, which connected to each other to assemble into the well-defined hierarchical SnO_2 microspheres.

The intrinsic structure of the as-prepared SnO_2 samples was further characterized with TEM. Figure 2c displays the typical TEM image of as-prepared SnO_2 sample (sample **I**) which also confirms the hierarchical microsphere structures. The HRTEM image (Figure 2d) taken from the edge of the microsphere clearly displayed the resolved lattice fringes of 0.333 nm, which corresponds to the (110) planes of rutile SnO_2 structure. The crystalline fringes imply the SnO_2 nanosheets are single crystalline. The diffraction spots in the SAED pattern (inset in Figure 2d) recorded on the edge of the SnO_2 microsphere also demonstrate the single crystal nature of the SnO_2 nanosheets which is in agreement with the HRTEM observations.

Hierarchical SnO_2 microspheres assembled from the nanosheets can be easily prepared via a seed layer and a hydrothermal

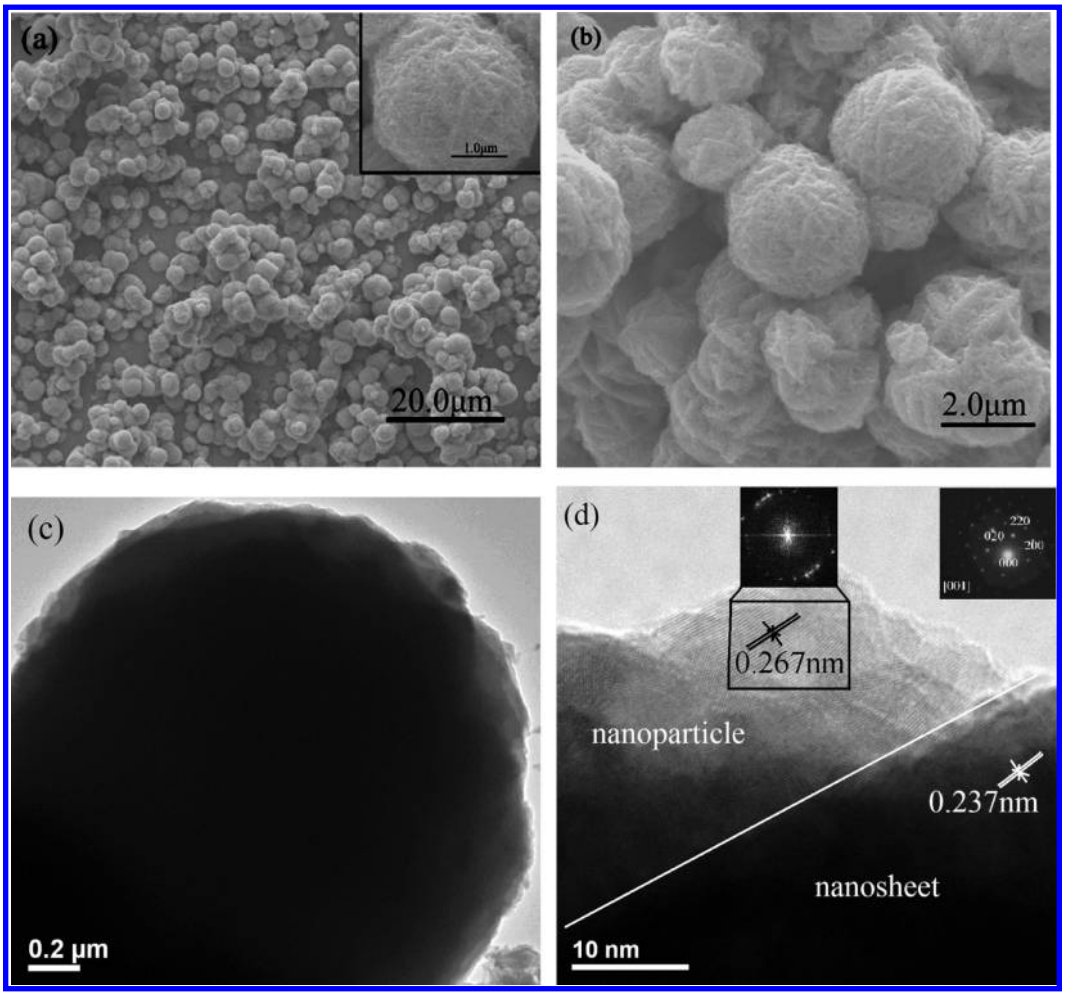

Figure 3. (a, b) FE-SEM images of sample **II** synthesized at 180 °C for 24 h with V_{H2O}:V_{acac} = 1:3, and (c) corresponding TEM image of a single microsphere, (d) HRTEM image of nanosheet (right bottom) and nanoparticle (left upper). Inset in Figure 3a is a higher magnification FE-SEM image. Inset in panel d are the SAED pattern (right upper) of the nanosheet and a FFT image of the nanoparticle (middle upper).

process. By carefully adjusting the experimental parameters, such as reaction temperature, reaction time, and the proper volume ratio of H_2O/acac, and so forth, hierarchical SnO_2 microspheres film with other interesting morphologies will be expected.

Figure 3 shows the FE-SEM and TEM images of sample **II** made at the H_2O:acac ratio of 1:3, keeping the other conditions the same as for sample **I** (hydrothermal temperature: 180 °C and hydrothermal time: 24 h). Lower magnification FE-SEM image (Figure 3a) shows the SnO_2 microspheres of about 3.0 μm, which are similar to sample **I**. However, close observation from the higher magnification FE-SEM image (Figure 3b) clearly disclose that the hierarchical SnO_2 microspheres are not only made up of nanosheets but also contained a number of nanoparticles. It is obvious from the inset in Figure 3a that the building units (nanosheets) of SnO_2 microspheres are not smooth where a lot of nanoparticles were homogenously coated on the surface. The present novel hierarchical SnO_2 microsphere films consisting of nanosheets and nanoparticles were further observed by a lower magnification TEM image (Figure 3c). The HRTEM image of an individual nanosheet and its SAED pattern reveal that both the nanosheet and the nanoparticle are single crystal, shown in Figure 3d. Furthermore, the corresponding Fast Fourier Transform (FFT) image (inset in Figure 3d, middle upper) also confirms the single crystal nature of nanoparticles.

From these SEM and TEM observations of samples **I** and **II**, we can conclude that the volume ratio of H_2O/acac has significant influence on the hierarchical SnO_2 structure. In the present system, the acac probably play the dual roles, not only as a solvent but also as a coordination reagent. Coordination of acac with the Sn^{4+} to form the Sn-acac-X (X: Cl or F) complex at adequate concentration (H_2O: acac = 1:1) induces slow hydrolysis reaction, probably facilitating formation of the nanosheets on the FTO glass substrate, which can be further assembled into the microspheres. At higher acac concentration (H_2O:acac = 1:3), more Sn-acac-X complexes than enough were formed, which may prevent additional Sn^{4+} from smooth conversion to SnO_2 nanosheets, but perhaps cause quite slow hydrolysis to further produce the nanoparticles on the surface of the nanosheets.

The effects of hydrothermal temperature on the final SnO_2 morphology were further investigated. When the reaction temperature increased to 200 °C (sample **III**), keeping the other experimental conditions the same as for sample **I**, FE-SEM results (Figure 4a) reveal that the hierarchical SnO_2 microspheres on the FTO glass substrate are made up of SnO_2 nanosheets. The size of the SnO_2 microsphere is about 4.0−5.0 μm in diameter and larger than that of sample **I**.

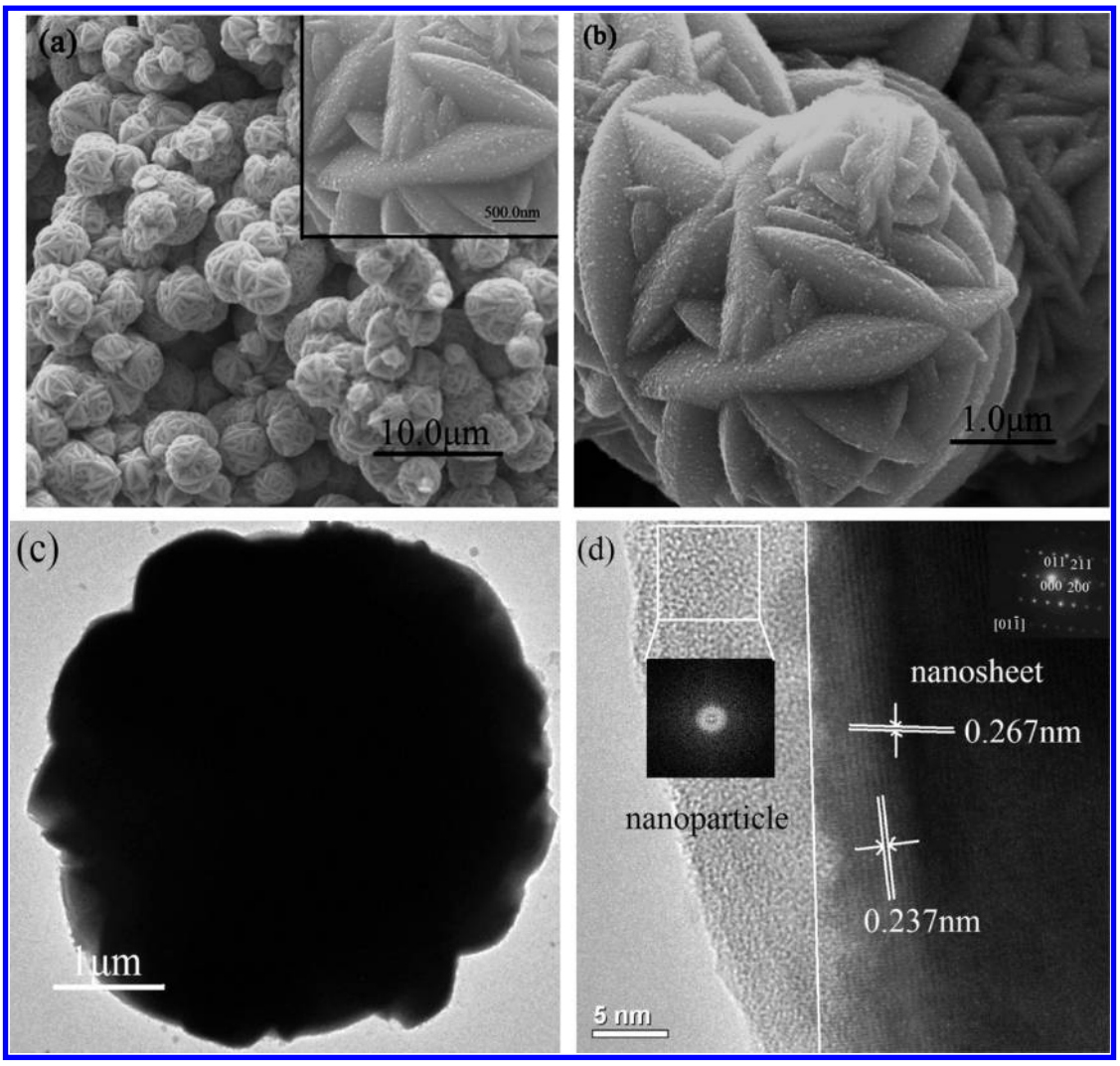

Figure 4. (a, b) FE-SEM images of sample **III** synthesized at 200 °C for 24 h with V_{H2O}:V_{acac} = 1:1, (c) corresponding TEM images of a typical SnO_2 microsphere, (d) HRTEM image of nanosheet and nanoparticle. Inset in Figure 4a is a higher magnification FE-SEM image. Insets in Figure 4d are SAED pattern, right upper and left middle correspond to nanosheet and nanoparticles, respectively.

A higher magnification SEM image clearly discloses that a number of nanoparticles coat onto the surface of the nanosheets which is different from sample **I** (Figure 2). The only difference between the samples **I** and **III** is the temperature; hence, it undoubtedly discloses that the hydrothermal reaction temperature strongly influences the morphology and structure of the final SnO_2 samples. Furthermore, the size of the nanoparticle is estimated to be 70−80 nm which is larger than that of sample **II** possessing 30 nm in nanoparticle size. This phenomenon implies that higher temperature will promote the growth of the SnO_2 nanosheets/nanoparticles resulting in the larger size of the final nanoparticles and microspheres. TEM image (Figure 4c) of sample **III** also reveals the microsphere structure of SnO_2 with 4.0−5.0 μm in diameter. The HRTEM image (Figure 4d) shows the SnO_2 nanosheets are single crystalline, and the distances of the lattice fringes were determined to be 0.267 and 0.237 nm, which can be indexed as (200) and (011) planes, respectively. SAED patterns of nanosheets also show the single crystal nature (inset in Figure 4d, right upper). However, the HREM and FFT patterns of nanoparticles reveal that they are of an amorphous nature (inset in Figure 4d, left). This is different from the above sample **II** (Figure 3) obtained at 180 °C with 1:3 ratio of H_2O/acac, where both nanoparticles and nanosheets are single crystalline.

To further explore the formation of the SnO_2 microspheres, time dependent experiments were carried out, and FE-SEM observations were used to trace the growth process. Panels a−e of Figures 5 display a series of interesting morphological evolutions of products synthesized at different hydrothermal periods of times (from 0.5 h to 48 h), keeping other experimental conditions the same as that of sample **I**. At the primary stage (0.5 h), the thick SnO_2 nanosheet or nanoparticle is observed (Figure 5a), which will assemble into the sphere-like or incomplete SnO_2 microsphere (1.2 μm in size) with the prolonged hydrothermal reaction time up to 2 h (Figure 5b). Irregular hierarchical SnO_2 microspheres are further formed when the reaction time is between 3 and 24 h, as shown in panels c and d of Figure 5 and Figure 2. These SEM results reveal that the size of the SnO_2 nanosheet and the microsphere increases with the increasing hydrothermal reaction time. Hence, on the basis of these SEM observations of different reaction times, the formation of hierarchical microsphere can be possibly ascribed to the self-assembly process of SnO_2 nanosheet during the hydrothermal process. With further increases in hydrothermal time (48 h), the hierarchical SnO_2

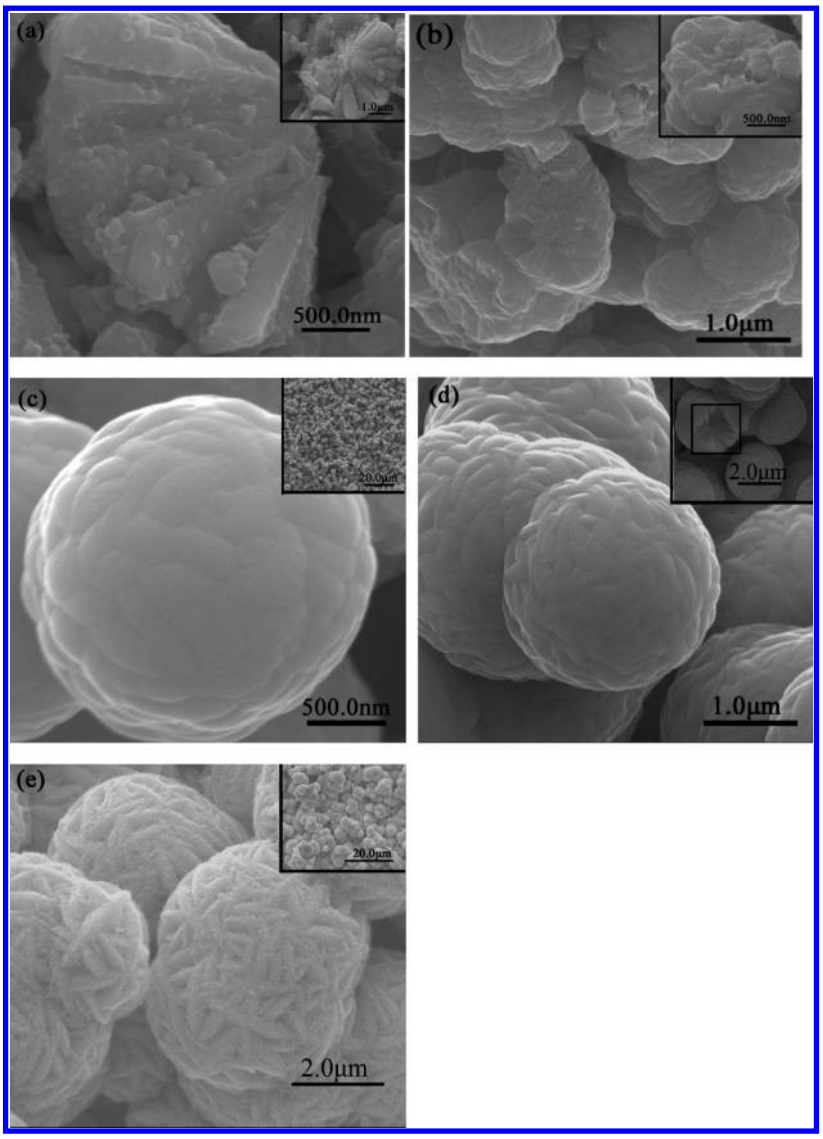

Figure 5. FE-SEM images of the SnO_2 microsphere synthesized at different hydrothermal time. Other experimental conditions are same as sample **I**. (a) 0.5 h, (b) 1 h, (c) 3 h, (d) 12 h, (e) 48 h. Insets are the corresponding low or high magnification FE-SEM images.

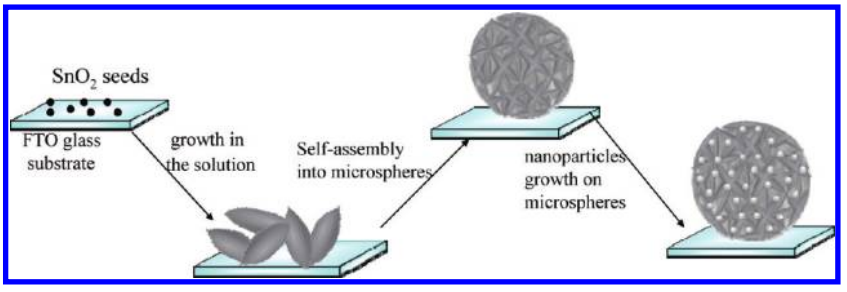

Figure 6. Schematic illustration of the growing process of hierarchical SnO_2 microspheres on FTO glass substrate.

microspheres with 4.0−5.0 μm in diameter are observed which are made up of nanosheets and a number of nanoparticles (Figure 5e). Interestingly, there are a number of nanoparticles that further grow on the surface of nanosheets/microspheres with the hydrothermal time longer than 24 h.

According to above discussions, the growth process of hierarchical SnO_2 microspheres is proposed and shown in Figure 6. First the SnO_2 precursors were coated onto the FTO glass as a seed layer via a dip-coating process. Under the assistance of acac and F^-, the SnO_2 seeds induce the growth of larger particles or nanosheets during the hydrothermal process. The cooperation synergistic effects of Sn-acac-X ($X = Cl^-$ or F^-) complex, acac, and F^- will promote the formation of nanosheets which then further assemble into microspheres. Furthermore, under higher temperature or higher acac content or longer hydrothermal time, additional SnO_2 nanoparticles will be formed and coated onto the surface of the nanosheets/microspheres. Finally, well-defined

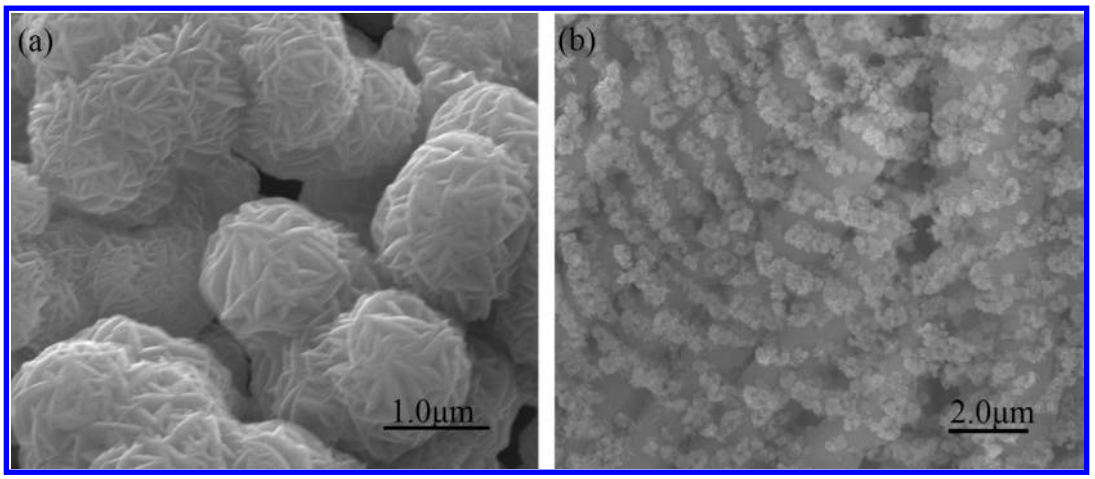

Figure 7. FE-SEM images of the SnO_2 microsphere synthesized at 180 °C for 24 h. (a) 40 mL H_2O (without acac), white precipitate is on the bottom of autoclave, (b) 40 mL acac (without H_2O), very little product on the FTO glass substrate.

Table 1. Size of Microspheres and Particles of Different Hierarchical SnO_2 Samples Made at Various Experimental Conditions

samples	size of microsphere	size of particle	note
sample **I**	2.0−2.5 μm	no particle	hierarchical microspheres consist of nanosheets, compact films on the FTO glass substrate
sample **II**	~3.0 μm	~30 nm	hierarchical microspheres consist of nanosheets and nanoparticles, compact films on the FTO glass substrate
sample **III**	4.0−5.0 μm	70−80 nm	hierarchical microspheres consist of nanosheets and nanoparticles, compact films on the FTO glass substrate
similar as sample **I**, only without acac	1.0−1.5 μm	no particle	hierarchical microspheres consist of thin nanosheets, white powder on the bottom of autoclave, no product on the FTO glass substrate

hierarchical SnO_2 microspheres films consisting of nanosheets and a number of nanoparticles on transparent FTO glass will be obtained via a facile hydrothermal process. According to the SEM/TEM observations, at a certain experimental conditions (180 °C, 1:1 ratio of H_2O/acac, 24 h), there may have been an equilibrium between SnO_2 nanosheets and Sn-acac-X complex during the hydrothermal process, which is favorable for the formation of nanosheets and microspheres on the FTO glass substrate. However, under higher temperature (200 °C) or larger acac concentration (volume ratio of H_2O:acac is 1:3) or longer hydrothermal time (48 h, 72 h), the equilibrium will be broken, resulting in the formation of additional nanoparticles on the surface of nanosheets/microspheres.

Both the seed layers and NH_4F are crucial for the growth of the hierarchical SnO_2 microspheres. One controllable experiment was performed while keeping the other conditions the same as for sample **I**, only without seed layers. After hydrothermal reaction, there were no products on the either the FTO glass surface or the autoclave bottom. It implied the seed layer played an important role for the formation of SnO_2 in the present experimental conditions. The SnO_2 seeds probably provide the growth points and induce the following growth of nanosheets/microspheres. Another two controllable experiments were performed in the absence of NH_4F or using NH_4Cl to replace NH_4F, keeping other experimental conditions the same as for sample **I**; no products were obtained on the FTO glass and the bottom of autoclave. It implies the NH_4F (exactly speaking, F^-) plays an important role in promoting the hydrolysis of Sn-acac-X (X = Cl^- or F^-) complex and formation of the SnO_2. However the exact role of NH_4F needs further investigations.

From the above results of sample **I** and sample **II**, the solvent ratio of H_2O/acac may have significant effects on the morphology of final samples. Here, a series of comparative experiments were further performed to observe the effect of acac content on the morphology of SnO_2 microspheres while keeping other conditions as sample **I**. In the absence of acac, namely, using 40 mL of H_2O, a white powder on the bottom of autoclave was obtained. No compact SnO_2 products on the FTO glass were observed. The formation of a white powder on the bottom of autoclave is probably due to the fast hydrolysis reaction in the absence of acac. There is a significant difference compared with sample **I** (H_2O:acac is 1:1), where a compact yellowish SnO_2 grew on the FTO glass surface under the assistance of Sn-acac-X (X = F, or Cl) owing to the slower hydrolysis reaction. Figure 7a shows the FE-SEM image of the white powder, which are hierarchical SnO_2 microspheres with 1.0−1.5 μm in diameter consisting of thin nanosheets. When a small quantity of acac was introduced into the system, for example, V_{H2O}:V_{acac} = 3:1 (data not shown) or 1:1 (sample **I**), the hierarchical SnO_2 microspheres films with larger diameter consisting of nanosheets on FTO glass were obtained (no product were formed on the bottom of autoclave), shown in Figure 2. The morphology and size of different samples are summarized in Table 1. As the acac content increased, V_{H2O}:V_{acac} = 1:3 (sample **II**), the hierarchical SnO_2 microsphere consisting of nanosheets and nanoparticles were formed, shown in Figure 4. However, in the absence of H_2O, namely, using 40 mL of acac, very little product was found on the FTO glass substrate, implying that the hydrolysis reaction happened with difficulty in the absence of water. Figure 7b shows the FE-SEM image of the SnO_2 samples prepared using 40 mL of acac, revealing that the samples were nanoparticles. Therefore, acac is found

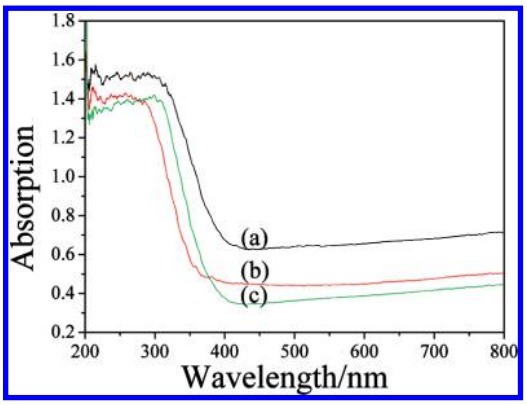

Figure 8. UV−vis diffuse reflectance spectra of SnO_2 microspheres after calcination at 500 °C for 3 h. (a) sample **I**, (b) sample **II**, and (c) sample **III**.

to influence strongly not only the crystal growth direction (see SAED and HRTEM images in Figure 2 and 3) but also the morphology of the final SnO_2 microsphere. The appropriate ratio between H_2O and acac is crucial for the final SnO_2 morphology and structures, which will result in different properties and applications.

UV−vis diffuse reflectance spectra data of material is related to the band gap which can be used to assert the structural variation. The present hierarchical SnO_2 microsphere films on FTO glass obtained at different conditions were further investigated by UV−vis measurements. Figure 8 presents the UV−vis spectra of samples **I**, **II**, and **III**; the corresponding absorption edges are around 430, 373, and 387 nm, respectively. Generally, the band gap value can be calculated via the equation of $E_g = 1240/\lambda$, where λ is the wavelength of the absorption edge. Hence, the band gap values of the present samples **I**, **II**, and **III** are 2.88, 3.32, 3.20 eV, respectively. The band gap of samples **II** and **III** shift to higher energy compared to that of sample **I**, which can be ascribed to SnO_2 microspheres consisting of a number of nanosized particles. It is well-known that the material with nanosized particles can result in a blue shift in the absorption wavelength. Moreover, sample **II** has a larger blue shift compared to sample **III** owing to better crystalline nature and smaller size of the nanoparticles for sample **II**. The size of nanoparticles and crystallines are 30 nm/ rutile and 70−80 nm/amorphous for samples **II** and **III**, respectively, as shown in Figures 3 and 4.

Conclusions

We have demonstrated the preparation of novel SnO_2 microspheres films on FTO glass substrate via a facile hydrothermal process. The cooperative effects of seed layer, NH_4F, and acac are believed to be responsible for the present novel hierarchical SnO_2 microspheres consisting of nanosheets and nanoparticles. And the hydrothermal reaction temperature, time, acac/H_2O ratio had significant influences on the SnO_2 morphology and hierarchical structure. Under higher temperature (200 °C), or longer hydrothermal reaction time, or larger acac/H_2O ratio, the SnO_2 particles with 30−80 nm in size covered on the surface of nanosheets/microspheres were successfully prepared, which would definitely increase the surface-to-volume ratio and have potential applications related to size and surface properties such as in catalysis, solar cells, sensors, and so forth.

Acknowledgment. The authors acknowledge financial support from the National Natural Science Foundation of China (20873183, U0934003), the Natural Science Foundation of Guangdong Province (8151027501000030), and the Foundation of Sun Yat-Sen University.